



**QUEEN'S
UNIVERSITY
BELFAST**

Evaluation of antimicrobial and anticancer activities of three peptides identified from the skin secretion of *Hylarana latouchii*

Lin, Y., Lin, T., Cheng, N., Wu, S., Huang, J., Chen, X., Chen, T., Zhou, M., Wang, L., & Shaw, C. (2021). Evaluation of antimicrobial and anticancer activities of three peptides identified from the skin secretion of *Hylarana latouchii*. *Acta Biochimica et Biophysica Sinica*. Advance online publication. <https://doi.org/10.1093/abbs/gmab126>

Published in:
Acta Biochimica et Biophysica Sinica

Document Version:
Peer reviewed version

Queen's University Belfast - Research Portal:
[Link to publication record in Queen's University Belfast Research Portal](#)

Publisher rights

Copyright The Author(s) 2021. Published by Oxford University Press on behalf of the Center for Excellence in Molecular Cell Science, Chinese Academy of Sciences.
This work is made available online in accordance with the publisher's policies. Please refer to any applicable terms of use of the publisher.

General rights

Copyright for the publications made accessible via the Queen's University Belfast Research Portal is retained by the author(s) and / or other copyright owners and it is a condition of accessing these publications that users recognise and abide by the legal requirements associated with these rights.

Take down policy

The Research Portal is Queen's institutional repository that provides access to Queen's research output. Every effort has been made to ensure that content in the Research Portal does not infringe any person's rights, or applicable UK laws. If you discover content in the Research Portal that you believe breaches copyright or violates any law, please contact openaccess@qub.ac.uk.

Open Access

This research has been made openly available by Queen's academics and its Open Research team. We would love to hear how access to this research benefits you. – Share your feedback with us: <http://go.qub.ac.uk/oa-feedback>

Original Article

Evaluation of antimicrobial and anticancer activities of three peptides identified from the skin secretion of *Hylarana latouchii*

Yan Lin^{1,2,*}, Tianxing Lin¹, Ningna Cheng¹, Shuting Wu³, Jiancai Huang³, Xiaoling Chen², Tianbao Chen², Mei Zhou², Lei Wang², and Chris Shaw²

¹College of Animal Sciences (College of Bee Science), Fujian Agriculture and Forestry University, Fuzhou 350002, China

²Natural Drug Discovery Group, School of Pharmacy, Queen's University, Belfast BT9 7BL, Northern Ireland, UK

³College of Chemistry, Fuzhou University, Fuzhou 350108, China

*Correspondence address. Tel. +86-18850138341; E-mail: ylin19@qub.ac.uk

Received: February 23, 2021

Editorial Decision: June 24, 2021

Running title: Peptides from *Hylarana latouchii*

Abstract

The skins of frogs of the family Ranidae are particularly rich sources of biologically-active peptides, among which antimicrobial peptides constitute the major portion. Some of these have attracted the interest of researchers because they possess both antimicrobial and anticancer activities. In this study, with “shotgun” cloning and MS/MS fragmentation, three antimicrobial peptides, homologues of family brevinin-1 (brevinin-1HL) and temporin (temporin-HLa and temporin-HLb), were discovered from the skin secretion of the broad-folded frog, *Hylarana latouchii*. They exhibited various degrees of antimicrobial and antibiofilm activities against test microorganisms, and haemolysis on horse erythrocytes. It was found that they could induce bacteria death through disrupting cell membranes and binding to bacterial DNA. In addition, they also showed different potencies towards human cancer cell lines. The secondary structure and physicochemical properties of each peptide were investigated to preliminarily reveal their structure-activity relationships. Circular dichroism spectrometry showed that they all adopted a canonical α -helical conformation in

membrane-mimetic solvents. Notably, the prepropeptide of brevinin-1HL from *H. latouchii* was highly identical to that of brevinin-1GHd from *Hylarana guentheri*, indicating a close relationship between these two species. Accordingly, this study provides candidates for the design of novel anti-infective and antineoplastic agents to fight multidrug-resistant bacteria and malignant tumours, and also offers additional clues for the taxonomy of ranid frogs.

Keywords: cloning, chromatography, mass spectrometry, structure-activity relationships

Introduction

Amphibians, having a rich evolutionary history and being the first group of organisms forming a connective link between aquatic and terrestrial environments, are confined to humid and/or moist habitats that are also the homes for a multitude of pathogenic microorganisms. Despite this and most surprisingly, they have existed and indeed thrived in such environments for several hundred millions of years with as many as 8343 extant species distributed worldwide (<https://amphibiaweb.org/index.html>, updated on 14 Jun. 2021). The ability to avoid invasion by pathogens has been attributed to their highly-evolved chemical immune defence system composed of various biological peptides. The specialised granular glands present in their skins play a vital role in such innate immunity and these structures synthesise, store and secrete a vast range of antimicrobial peptides (AMPs) which are employed on the skin surface following injury or stress, protecting them from the microbes they encounter [1].

Anuran skin has been found to be an exceedingly rich source of AMPs with diverse structures that contain no single conserved structural motif responsible for their activities [2]. However, almost without exception, they are characterised by their cationicity, hydrophobicity, and amphipathic α -helical configuration in membrane-mimetic solvents [3]. As components of the innate immune system, AMPs target a wide range of microorganisms, including bacteria, protozoa, fungi and viruses, and some recent studies has reported that many of these peptides also possess cytotoxicity against tumour cells [4–7].

Non-small cell lung cancer (NSCLC), the most common type of lung cancer (80%–90%), is one of the most fatal malignancies throughout the world with only 15%-20% of 5-year survival [8,9]. The failure in the treatment results from drug

resistance and delayed diagnosis. Recently, AMPs have attracted much attention as potential alternatives to antimicrobial or anticancer drugs due to their advantages over currently-used antibiotics and antitumour chemotherapeutic agents, including more selective cytotoxicity towards target cells, the capability of bypassing common multidrug-resistance mechanisms and their synergistic effects in combination therapy [10]. Although the exact molecular mechanisms of antimicrobial and anticancer actions of AMPs still remain obscure, many AMPs are deemed to share a common membranolytic mode of action in which these cationic peptides preferentially bind to the anionic components on bacterial/cancer cell membranes via electrostatic interaction, inducing membrane disruption that leads to cell death [11–14]. Some other mechanisms are also proposed for their anticancer action, such as intracellular calcium mechanisms, mitochondrial membrane disruption, induction of apoptosis and acting on chromosomes or nucleic acids [15–17].

H. latouchii is defined as a species under the genus *Hylarana* belonging to the Ranidae family. To date, although thousands of AMPs have been identified from amphibians, only 17 AMPs from *H. latouchii* belonging to families of brevinin-1, brevinin-2, esculentin-1, esculentin-2, temporin, nigrocin, palustrin-2, and hylaranin are deposited in the Antimicrobial Peptide Database (APD3).

In the present study, three AMPs were obtained from the skin secretion of *H. latouchii*, through “shotgun” cloning and MS/MS fragmentation of the skin secretion. Sequence characterisation indicated that they belong to two different peptide families (brevinin-1 and temporin family), they were named accordingly as brevinin-1HL, temporin-HLa and temporin-HLb. Antimicrobial, antibiofilm, haemolytic and antitumour cell assays were carried out to assess their biological activities towards test microorganisms and human cancers using their respective synthetic replicates. The mechanisms of their antimicrobial actions were also explored.

Materials and Methods

Collection of skin secretion from *H. latouchii*

Skin secretion was harvested from the specimens of adult *H. latouchii* captured in Fujian Province, China, by stimulating the dorsal skin surface with mild electricity as previously described [18]. The skin secretion, rinsed off with deionised water, was collected, lyophilised and stored at -20°C prior to use. The study was performed

according to the guidelines in the UK Animal (Scientific Procedures) Act 1986, project license PPL 2694, issued by the Department of Health, Social Services and Public Safety, Northern Ireland. All experimental procedures were vetted by the Institutional Animal Care and Use Committee (IACUC) of Queen's University Belfast and approved on 1 March, 2011.

“Shotgun” cloning of peptide precursor-encoding cDNAs

The full-length peptide precursor-encoding cDNAs were obtained from the *H. latouchii* skin secretion-derived cDNA library as previously described [19]. Briefly, cDNA library constructed from polyadenylated mRNA was subject to 3'-RACE procedures employing a NUP primer (Clontech, Oxford, UK) and a degenerate sense primer (5'-GAWYYAYYHRAGCCYAAADATGTTCA-3') designed to a highly-conserved domain within the 5'-untranslated region of ranid frogs' AMP precursor cDNAs [20].

Identification and structure characterisation of antimicrobial peptides

H. latouchii skin secretion was isolated by reverse phase HPLC equipped with a Jupiter C-5 semi preparative column (25 cm × 1 cm; Phenomenex, Torrance, USA), and the primary structures of putative cDNA-encoded peptides present in the HPLC fractions were analysed by the MS/MS fragmentation sequencing using an LCQ Fleet ESI ion-trap mass spectrometer (Thermo Fisher Scientific, Waltham, USA) as previously described [19].

Peptide synthesis

Following the establishment of peptide primary structures on the basis of cloned cDNAs and MS/MS analyses, each peptide was chemically synthesised using a PS3 automated solid-phase synthesiser (Protein Technologies, Inc., Tucson, USA). Reverse phase HPLC was used to purify the synthesised peptides whose purity and authenticity were then confirmed by matrix-assisted laser desorption/ionisation time-of-flight mass spectrometry (MALDI-TOF MS) and MS/MS fragmentation sequencing.

Secondary structure analyses and prediction of physicochemical properties of

antimicrobial peptides

The peptide secondary structures were analysed using a Bio-Logic MOS-450 circular dichroism (CD) spectrometer (Bio-Logic, Seyssinet-Pariset, France) as previously described [5,21] with some modifications. Each peptide was dissolved in ultrapure water and a 50% trifluoroethanol (TFE) solution, respectively, at a concentration of 40 μM , in a 2-mm high precision quartz cell. CD spectra were obtained at room temperature from 185 nm to 250 nm with acquisition duration of 0.5 s. Data are expressed as the mean residue ellipticity ($[\theta]$, $\text{deg cm}^2 \text{dmol}^{-1}$) calculated from the equation: $[\theta] = (\theta_{\text{obs}} \times 1000) / (c \times l \times n)$, where θ_{obs} is the observed ellipticity (mdeg), c is the peptide concentration (μM), l is the path length (mm), and n is the number of amino acids [22].

The α -helical wheel plots, hydrophobicity, and hydrophobic moments of peptides were obtained via Heliquest [23]. The net charge of peptides at neutral pH was determined using the Innovagen peptide property calculator (<https://www.pepcalc.com/ppc.php>). The prediction of 3D models of peptides was performed on a I-TASSER online server (<https://zhanglab.ccmb.med.umich.edu/I-TASSER/>) [24].

Antimicrobial assay

The antimicrobial activity of peptides was measured against the Gram-negative bacteria, *Escherichia coli* (*E. coli*) (NCTC10418), *Pseudomonas aeruginosa* (*P. aeruginosa*) (ATCC27853) and *Chromobacterium violaceum* (*C. violaceum*) (ATCC12472); the Gram-positive bacteria, *Staphylococcus aureus* (*S. aureus*) (NCTC 10788), methicillin-resistant *S. aureus* (MRSA) (ATCC 43300) and *Enterococcus faecalis* (*E. faecalis*) (NCTC 12697); and the yeast, *Candida albicans* (*C. albicans*) (NCPF1467), as previously described [25]. Briefly, cultures of model microorganisms were diluted to 1×10^6 colony-forming units (cfu)/ml and incubated with peptide solutions in the range of 1-512 mg/l overnight. The lowest concentration at which no growth of microorganism was detectable at 550 nm was considered as minimum inhibitory concentration (MIC). Then, minimum bactericidal concentration (MBC) was determined by inoculating 10 μl of medium from clear wells onto the Mueller Hinton agar (MHA) plates, which showed no growth of colony after 24 h of incubation.

Antibiofilm assay

The antibiofilm activity of peptides was evaluated by the minimum biofilm inhibitory concentration (MBIC) and the minimum biofilm eradication concentration (MBEC) assays against *S. aureus* and *P. aeruginosa* as previously described [26,27] with some modifications. For the MBIC assay, 1×10^6 cfu/ml bacterial culture in Mueller-Hinton Broth (MHB) was mixed with antimicrobial peptides (1-512 mg/l) in a 96-well plate, followed by incubation for 24 h at 37°C at 120 rpm. For the MBEC assay, the same density of bacterial culture was grown in a 96-well plate for 24 h at 37°C at 120 rpm, to form the biofilms. The plate was then washed with sterile PBS to remove planktonic bacteria, and peptides (1-512 mg/l) were added, followed by 24 h of incubation at 37°C and 120 rpm. After being washed with PBS to remove planktonic and dead bacteria, the plate was incubated again for 24 h at 37°C at 120 rpm, in the presence of MHB (200 µl), to enhance the formation of the existing biofilms. Before measuring the absorbance at 595 nm in an Infinite F50 plate reader (Tecan, Männedorf, Switzerland), the formed biofilms at the bottom of both the MBIC and MBEC plates were washed twice with PBS, fixed with 200 µl of methanol for 10 min, stained with 200 µl of crystal violet (1%; w/v) for 10 min, and dissolved in 200 µl of acetic acid (33%; v/v) for 60 min.

Haemolysis assay

The haemolytic activity of peptides was examined in horse erythrocytes using a series of peptide concentrations from 1 to 512 mg/l as described previously [25], where erythrocytes treated with 1% (v/v) Triton X-100 and sterile PBS were used as positive control (100% haemolysis) and negative control (0% haemolysis), respectively. The peptide concentration for 50% haemolysis (HC₅₀) was calculated using the best-fitted curve.

SYTOX Green uptake assay

The permeabilisation effects of peptides on the Gram-positive bacterial membrane were evaluated by SYTOX Green uptake assay as described previously [28] with minor modifications. *S. aureus* grown to the logarithmic phase was suspended in HEPES buffer (Solarbio, Shanghai, China) to obtain the concentration of 1×10^8

cfu/ml, followed by incubation with peptides (1 × MICs, 2 × MICs and 4 × MICs) and 1 μM SYTOX™ Green Nucleic Acid Stain (Invitrogen, Carlsbad, USA). Triton X-100 (1%; v/v) and sterile HEPES were regarded as positive control and negative control, respectively. Melittin (1 × MICs, 2 × MICs and 4 × MICs; MedMol, Shanghai, China) was also tested for comparison. The fluorescence intensity was monitored every minute at 37°C in a Varioskan™ LUX microplate reader (Thermo Scientific) with the excitation and emission wavelengths of 485 nm and 528 nm over 60 min.

Inner membrane and outer membrane permeability assays

The effects of peptides on the bacterial inner membrane (IM) permeability were assessed on *E. coli* on the basis of the conversion from colourless *o*-nitrophenyl-β-D-galactopyranoside (ONPG) to yellow *o*-nitrophenol by β-galactosidase released from membrane-destroyed bacteria [21]. Peptides at the concentrations of 1 × MICs, 2 × MICs and 4 × MICs were incubated with 30 mM ONPG (Beyotime, Shanghai, China) and 1 × 10⁸ cfu/ml bacterial culture at logarithmic phase. Triton X-100 (1%; v/v) and sterile PBS were regarded as positive control and negative control, respectively. Melittin (1 × MICs, 2 × MICs and 4 × MICs) was also tested for comparison. The absorbance was monitored every 5 min at 420 nm and 37°C in a Multiskan™ FC microplate reader (Thermo Scientific) over 150 min.

The effects of peptides on the bacterial outer membrane (OM) permeability were assessed on *E. coli* by the N-phenyl-1-naphthylamine (NPN) uptake assay as previously described [21,29]. Peptides at the concentrations as above were incubated with 10 μM NPN (Solarbio) and 1 × 10⁸ cfu/ml bacterial culture at logarithmic phase. Polymyxin B (32 mg/l; Solarbio) and sterile PBS were regarded as positive control and negative control, respectively. Melittin (1 × MICs, 2 × MICs and 4 × MICs) was also tested for comparison. The fluorescence intensity was monitored every 10 min at 37°C in a Varioskan™ LUX microplate reader (Thermo Scientific) with the excitation and emission wavelengths of 350 nm and 420 nm over 60 min. The membrane permeability rate is expressed as $\text{NPN uptake (\%)} = (F - F_0) / (F_{\text{max}} - F_0) \times 100\%$, where F is the fluorescence intensity of bacterial culture treated with peptides, F₀ and F_{max} are that treated with PBS and polymyxin B, respectively.

Scanning electron microscopy (SEM)

The effects of peptides on the morphology and membrane integrity of *E. coli* and *S. aureus* were examined directly with SEM as previously described [30]. Logarithmic phase bacteria resuspended in PBS at the concentration of 1×10^8 cfu/ml were treated with peptides ($0.5 \times$ MICs and $0.25 \times$ MICs) or vehicle alone (negative control) for 18 h at 37°C. The bacterial cells were then subject to fixation, dehydration and coating with gold-palladium prior to the observation with a JSM-6380LV scanning electron microscope (JEOL, Tokyo, Japan).

DNA binding assay

The capability of peptides to bind to the bacterial genomic DNA was assessed by gel retardation assay as previously described [31]. Genomic DNA of *E. coli*, *P. aeruginosa*, *S. aureus*, MRSA and *E. faecalis* was extracted using a Bacterial Genomic DNA Extraction kit (TIANGEN, Beijing, China), followed by incubation with peptide solutions (2-512 mg/l) for 5 h at 37°C. Samples were analyzed by agarose gel electrophoresis (5% agarose gel), and were then visualised using a JS-6800 UV trans-illuminator (Peiqing Science and Technology, Shanghai, China).

Cell culture and anticancer proliferative assays

The inhibitory activity of peptides on the proliferation of representative human cancer cell lines was evaluated by MTT assay. Prostate cancer cells, DU145 (ATCC, Rockefeller, USA; HTB-81), PC3 (ATCC; CRL-1435) and LNCaP (ATCC; CRL-1740); lung cancer cells, NCI-H838 (ATCC; CRL-5844), NCI-H23 (ATCC; CRL-5800), NCI-H157 (ATCC; CRL-5802) and NCI-H460 (ATCC; HTB-177); breast cancer cells, MDA-MB-231 (ATCC; HTB-26), MDA-MB-435s (ATCC; HTB-129) and MCF-7 (ATCC; HTB-22); and neurospongioma cells, U251-MG (ECACC, Uppsala, Sweden; 09063001), were cultured in Gibco® RPMI-1640 medium (Invitrogen) or Dulbecco's modified Eagle's medium (DMEM; Invitrogen) with 10% foetal bovine serum (FBS; Sigma, St Louis, USA) and 1% penicillin-streptomycin solution (Sigma) in an incubator containing 5% CO₂ at 37°C. In brief, cells (5×10^3 cells/well, 100 µl) were grown in 96-well plates for 24 h prior to the 12-h starvation and treatment with peptide solutions (10^{-12} to 10^{-4} M) for 24, 48

and 72 h. Cells treated with serum-free medium and melittin (10^{-5} M) served as negative control and positive control, respectively. Then, 10 μ l of MTT solution (5 mg/ml; Sigma) was added to each well for a further 4-h incubation, after which the formed formazan crystals were dissolved in 100 μ l of DMSO and the absorbance was measured at 550 nm in a Synergy HT plate reader (Bio Tek, Winooski, USA). Cell viability is expressed as the absorbance of cells treated with peptides relative to those treated with medium. The peptide concentration for 50% inhibition of cell growth (IC_{50}) was calculated using the best-fitted curve.

Statistical analysis

All the biological evaluation assays were repeated at least three times with seven replicates in each independent test. The statistical analysis was performed with GraphPad Prism 5.0 software (San Diego, USA), in which one-way ANOVA analysis was used and $P < 0.05$ was considered to be statistically significant. Data were presented as the mean \pm SEM.

Results

“Shotgun” cloning of putative antimicrobial peptide precursor-encoding cDNAs

Using the “shotgun” cloning strategy, three full-length cDNAs encoding three different peptide precursors were obtained from the *H. latouchii* skin secretion-derived cDNA library

A

```

      M F T L K K S L L L L F F L G T I
1  ATGTTACCT TGAAGAAATC CCTGTACTC CTTTCTTCC TTGGGACCAT
      · N L S F C E E E R N A D E E E R R
51 CAACTTATCT TTCTGTGAGG AAGAGAGAAA TGCTGATGAG GAAGAAAGAA
      · D D P D K M D A E V Q K R F L G
101 GAGATGATCC CGATAAAATG GATGCTGAAG TGCAAAAACG ATTTTGGGA
      A L F K V A S K L V P A A I C S I
151 GCGTTGTCA AGGTGGCTTCAAATTAGTA CCAGCAGCTA TTTGTTCAAT
      · S K K C *
201 TTCTAAAAA TGTTGAAGCT TTGAAATGA AAATCGTCTG AAGTGAATA
251 TCATTTAGCT AAATGCACAT CAGATGACTT TAAAAAATA AACATGTTGC
301 ATACACAAAA AAAAAAAAAA AAAAAAAAAA AAAAA

```

B

```

      M F T L K K S L L L L F F L G A I
1  ATGTTACCT TGAAGAAATC CCTGTACTC CTTTCTTCC TTGGGGCCAT
      · N L S L C Q E E R N A E E E R R D
51 CAACTTATCT CTCTGTGAGG AAGAGAGAAA TGCGGAAGAA GAAAGAAGAG
      · G D D E R A V E V N K R F F P L
101 ATGGTGATGA TGAAAGGGCT GTTGAAGTGA ACAAACGATT TTTCCGCTT
      I F G A L S S I L P K I L G K *
151 ATTTTGGTG CGCTCAGTAG CATTGTTGCA AAAATTTGG GAAAATAACC
201 AAAAAATGTT GAAACTTTGG AAATGGAAAT CATCTGAGGT GGAATATCAT
251 TTAGTTTAAT GCACATCAGA TGTCTTAAAA ATAAAGATAT TACATTGTGA
301 GAAAAAAAAA AAAAAAAAAA AAAAAAAAAA

```

C

```

      M F T L K K S L L L L F F L G T I
1  ATGTTACCT TGAAGAAATC CCTGTACTC CTTTCTTCC TTGGGACCAT
      · N L S L C E E E R N A D V E E R R
51 CAACTTATCT CTCTGTGAGG AAGAGAGAAA TGCGATGTG GAAGAAAGAA
      · D G D D Q E A V E V N K R F L Q
101 GAGATGGTGA TGATCAAGAG GCTGTGGAAG TGAACAAAAG ATTTTACAG
      H I I G A L S H I F G K *
151 CATATTATTG GCGCGCTCAG TCATATTTTT GGAAAATGAC CAAAAATAT
201 TGAAACTTTG GAAATGGAAA TCATCTGATG TAGAATATCA TTTAGCTAAG
251 TGCACATCAG ATGTCTTATA AAAAATAAAG ATGTTGAAGA AAAAAAAAAA
( 301 AAAAAAAAAA AAAAA

```

Figure 1). The open-reading frames of the precursors consisted of 71, 65 and 62 amino acid residues, respectively, each containing a single copy of respective 24-mer, 17-mer and 13-mer mature peptides. Domain topology of these biosynthetic precursors revealed that they were made up of highly-conserved putative signal peptides, acidic amino acid residue-rich spacer peptides that terminate in a classical propeptide convertase cleavage site (-KR-), and different C-terminal mature peptides

(**Figure 2A**). Bioinformatic investigations of the deduced mature peptides were performed using the NCBI BLASTp programme, which indicated that one belonged to brevinin-1 family and the other two belonged to temporin family; hence, they were named brevinin-1HL, temporin-HLa and temporin-HLb (HL = *Hylarana latouchii*) accordingly. Specifically, brevinin-1HL was typified by a canonical disulphide-bridged loop, the so-called “Rana box”, at the C-terminus, and through BLAST search, it was the most homologous to *Hylarana guentheri* brevinin-1GHd (100%) and brevinin-1GHa (83%), as well as *Rana rugosa* gaegurin 5 (71%; **Figure 2B**). Interestingly, the prepropeptide sequences of brevinin-1HL and brevinin-1GHd showed only one amino acid substitution within the signal peptide domain (**Figure 2C**). Temporin-HLa and temporin-HLb were flanked C-terminally by a Gly residue and a basic amino acid (Lys), which implied that Lys would be removed by carboxypeptidase during processing to expose the extra-Gly residue serving as an amide donor for the C-terminal amidated residue of respective mature peptides [32]. According to the BLAST analyses, temporin-HLa showed 76% structural similarity to temporins from *Hylarana* frogs, including temporin-RNs from *Hylarana nigrovittata*, and temporin-LTa from *Hylarana latouchii* (**Figure 2D**). Temporin-HLb presented the highest structural identity with temporin-GHc (92%), -GHd (92%) and -GHa (85%) from *Hylarana guentheri* (**Figure 2E**). The cDNA sequences of brevinin-1HL, temporin-HLa and temporin-HLb have been deposited in the EMBL Nucleotide Sequence Database with the accession codes of LT891928, LT891929 and LT891930, respectively.

Isolation and structural characterisation of deduced peptides from the skin secretion of *H. latouchii*

Based on the predicted molecular masses from the cloned precursors and the compensation for post-translational modification (C-terminal single disulphide bridge formation and α -amidation resulted in deduction of 2 Da and 1 Da, respectively), each mature peptide was identified in different HPLC fractions of skin secretion by MALDI-TOF MS (**Figure 3** and Error! Reference source not found.). The primary structures of respective peptides were confirmed by MS/MS fragmentation sequencing (**Figure 4**).

Chemical synthesis, secondary structure analyses and physicochemical properties of peptides

Brevinin-1HL, temporin-HLa and temporin-HLb were successfully synthesised, and were purified using reverse phase HPLC. Their purity and sequence were confirmed by MALDI-TOF MS and MS/MS fragmentation analysis.

CD spectrometric analyses revealed that brevinin-1HL, temporin-HLa and temporin-HLb presented a random coil structure in the aqueous solution with a negative band at 200 nm (**Figure 5A**), while they adopted a typical α -helical structure in the membrane-mimicking 50% TFE solution with a positive band at 192 nm and negative bands at 208 and 222 nm (**Figure 5B**), which is the canonical spectrum of α -helix.

Prediction of the secondary structures and 3D models of the peptides by an online server indicated that each peptide had a potential propensity for α -helix formation (**Figure 6**), which is consistent with the CD spectrometric analyses (**Figure 5**). The helical wheel projection revealed an amphipathic nature with hydrophobic residues positioning on one side of the helical axis, while hydrophilic residues were positioned on the opposite side (**Figure 6**). The primary structures, secondary structure predictions and physicochemical properties, including predicted net charge, hydrophobicity, and relative hydrophobic moments of each peptide and their analogues discovered in previous studies [33–37] are summarised in Error! Reference source not found., which shows that all peptides share a cationic and amphipathic property with a certain degree of α -helix.

Antimicrobial and haemolytic activities of peptides

The MIC and MBC values and the haemolytic effects of peptides towards the test microorganisms as well as horse erythrocytes are shown in Error! Reference source not found. and **Figure 7**. Brevinin-1HL exhibited broad-spectrum antimicrobial activity against the model microorganisms except *C. violaceum* with MIC values of 3.2-102.6 μ M and also exhibited bactericidal activity against some microorganisms (*E. coli*, *S. aureus* and *C. albicans*) with MBC values of 12.8-51.3 μ M, but at the same time, it had considerable cytotoxicity on horse erythrocytes, causing 86.8% of haemolysis at 102.6 μ M. Temporin-HLa was only potent against the Gram-positive bacteria, *S. aureus* and *E. faecalis*, and the yeast, *C. albicans*, with MICs/MBCs

between 8.5 and 68.3 μM . It showed moderate haemolytic activity with an HC_{50} value of $31.4 \pm 0.7 \mu\text{M}$. In contrast, temporin-HLb was virtually ineffective against almost all test microorganisms but specifically inhibited the growth of *S. aureus* with an MIC of 10.7 μM . It could not kill this bacterium even at a concentration up to 343 μM . However, it had extremely weak haemolytic activity (1%) at the MIC value. The antimicrobial results of the three peptides and haemolytic result of melittin are shown in **Supplementary Figs. S1,2**.

Antibiofilm activity of peptides

As shown in Error! Reference source not found., brevinin-1HL could inhibit the formation of *P. aeruginosa* and *S. aureus* biofilms with MBIC values of 25.7-102.6 μM , while it only had the ability to eliminate the mature biofilm of *S. aureus*. Temporin-HLa and temporin-HLb could also suppress the biofilm formation in *S. aureus* with MBICs of 17.1 μM and 21.4 μM , but they did not eradicate the previously formed biofilms. The antibiofilm results of peptides, including melittin, are shown in **Supplementary Figs. S3,4**.

Membrane permeabilisation capability of peptides on Gram-positive bacteria

The permeabilisation effects of peptides on the membrane of *S. aureus* were evaluated by SYTOX Green uptake assay (

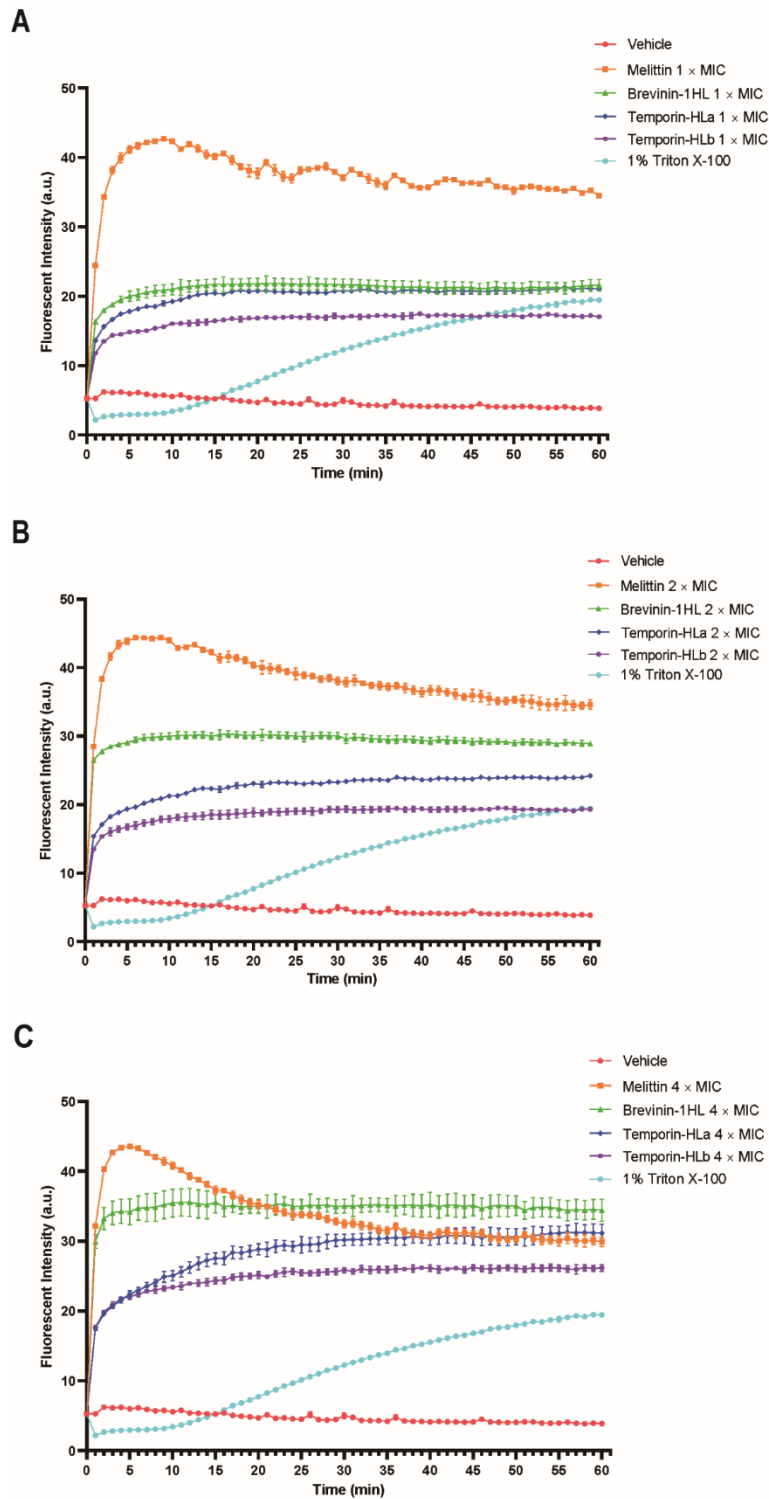


Figure 8). The time course of membrane permeability indicated that, compared with 1% Triton X-100, brevinin-1HL, temporin-HLa and -HLb disrupted the cell membrane promptly in 5 min at 1-, 2- and 4-fold MICs. They showed a dose-dependent membrane permeabilisation ability with the order of brevinin-1HL > temporin-HLa > temporin-HLb. However, even at the highest concentrations (4 × MICs), their disruptive potencies were weaker than that of melittin which destroyed

the cell membrane completely in 10 min at $1 \times \text{MIC}$.

Membrane permeabilisation capability of peptides on Gram-negative bacteria

As brevinin-1HL displayed antimicrobial activity towards Gram-negative bacteria, its ability to disrupt the outer and plasma membranes were assessed on *E. coli*. **Figure 9A** showed that brevinin-1HL disrupted the integrity of inner membrane in dose- and time-dependent manners, with a stronger potency than 1% Triton X-100. Although melittin ($2 \times \text{MIC}$ and $4 \times \text{MIC}$) showed a slightly higher disruptive capability in 60 min, the efficacy of brevinin-1HL ($4 \times \text{MIC}$) surpassed it after that.

Similar to the effects on the inner membrane, brevinin-1HL dose- and time-dependently destroyed the outer membrane of *E. coli*. Notably, the disruptive efficacies of the tested concentrations of brevinin-1HL ($1 \times \text{MIC}$, $2 \times \text{MIC}$ and $4 \times \text{MIC}$) were much stronger than those of melittin (**Figure 9B**).

Effects of peptides on the morphology of bacteria

The membrane integrity and morphology of *E. coli* and *S. aureus* treated with peptides were observed directly by SEM. Obviously, control cells presented a plump shape with a smooth and integral surface (**Figure 10A,B**). On the other hand, both strains of bacteria displayed distinctly rough, shrunk, irregular and even corrupted surfaces and shapes after treatment with each peptide (**Figure 10C-J**). The destructive efficacies were in a dose-dependent manner. Among the three AMPs, brevinin-1HL was the most harmful, as revealed by inclusive leakage which indicated severe cell lysis (**Figure 10C-F**).

DNA binding ability of peptides

The DNA binding ability of each peptide to the corresponding sensitive microbes was evaluated. As shown in **Figure 11A-E**, brevinin-1HL could only bind to the DNA of *S. aureus*, MRSA and *E. faecalis* at the highest tested concentration ($205.2 \mu\text{M}$). Temporin-HLa possessed a distinct DNA binding ability to *S. aureus* at the concentrations higher than $68.3 \mu\text{M}$ (**Figure 11F**). On the contrary, temporin-HLb had no such ability (**Figure 11H**).

Anti-proliferative effects of peptides on human cancer cell lines

The anti-proliferative effects of brevinin-1HL, temporin-HLa and temporin-HLb on a series of human cancer cell lines were examined. Brevinin-1HL demonstrated preferential cytotoxicity towards H23 cells with an IC₅₀ around 8 µM. The results of the treatment of H23 cells with brevinin-1HL for 24, 48 and 72 h are graphically presented in **Figure 12A**. Temporin-HLa was active in some lung cancer cell lines tested with IC₅₀ values of 1-15 µM. The results of the treatment of H23, H157 and H460 cells with temporin-HLa for 24, 48 and 72 h are graphically presented in **Figure 12B-D**. Both brevinin-1HL and temporin-HLa induced corresponding cell death in a dose-dependent manner and regardless of the duration of treatment, no distinct difference in toxicity was observed, which meant that these two peptides could exert their greatest anticancer effects in the first 24 h. The IC₅₀ values of peptides towards relevant cells are listed in Error! Reference source not found.. Data for the ineffective results are not shown.

Discussion

In the past several decades, as important components of the innate immune system, thousands of AMPs have been discovered in plants, insects, vertebrates including humans, as well as in many microorganisms [38,39]. The skins of amphibians, especially those of ranid frogs [40], have been found to contain abundant and unique glands that secrete a vast number of biologically-active compounds which form an excellent protective barrier against coexisting predators and pathogenic microorganisms in their habitats. Among these various molecular categories present in the secretions, peptides represent the predominant category with numerous bioactivities falling into pharmacological and antimicrobial types [41]. Some of the AMPs have broad-spectrum antimicrobial activity without observable cytolytic activity against normal mammalian cells [42,43]. Although the precise antimicrobial mechanism is not completely understood, the most widely-accepted mechanism is through rapid membrane-disruption that can only cause resistance with great difficulty. This is quite different from conventional antibiotics that kill microbes through interaction with specific and discrete molecular targets [44,45]. These features make AMPs of potential value as therapeutic agents for the treatment of infections caused by multidrug-resistant pathogens.

In the present study, three AMPs (brevinin-1HL, temporin-HLa and temporin-HLb)

were identified in the skin secretion of the broad-folded frog, *H. latouchii*. With regard to their antimicrobial activities, brevinin-1HL possessed a relatively broad-spectrum activity, while temporin-HLa and -HLb were only specifically effective against some Gram-positive bacteria or fungi. The MICs of brevinin-1HL against Gram-negative bacteria were generally higher than those against Gram-positive strains (Error! Reference source not found.). This phenomenon was also found in other AMPs that Gram-negative bacteria tended to be more difficult to be damaged due to the extra outer membrane that could trap AMPs, extend folding and facilitate helical oligomeric formation [46]. In particular, the aromatic sidechain of Phe at the N-terminus and the hydrophobic residues in the middle of temporin-HLa and -HLb might induce the formation of oligomeric structures on the outer membrane, preventing their entry to the inner membrane, resulting in ineffectiveness against Gram-negative bacteria [5,46].

As biofilms have been a tremendous problem for the treatment of many human infections owing to the insusceptibility to antimicrobial agents and severe pathogenesis [47], the antibiofilm activities of peptides were assessed on *P. aeruginosa* and *S. aureus*. Basically, sessile communities of microbes are more self-protected and more resistant to antibacterial agents than the planktonic state because biofilms are formed by the accumulation of microorganisms and production of extracellular polysaccharides [48]. Hence, as expected, compared with MBCs, MBECs of peptides were higher, or even beyond the tested concentrations (Error! Reference source not found.,4).

To preliminarily investigate the mechanisms of antimicrobial actions of these three peptides, their membrane permeabilisation and DNA binding capabilities were studied. As shown in the dynamic-course figures (

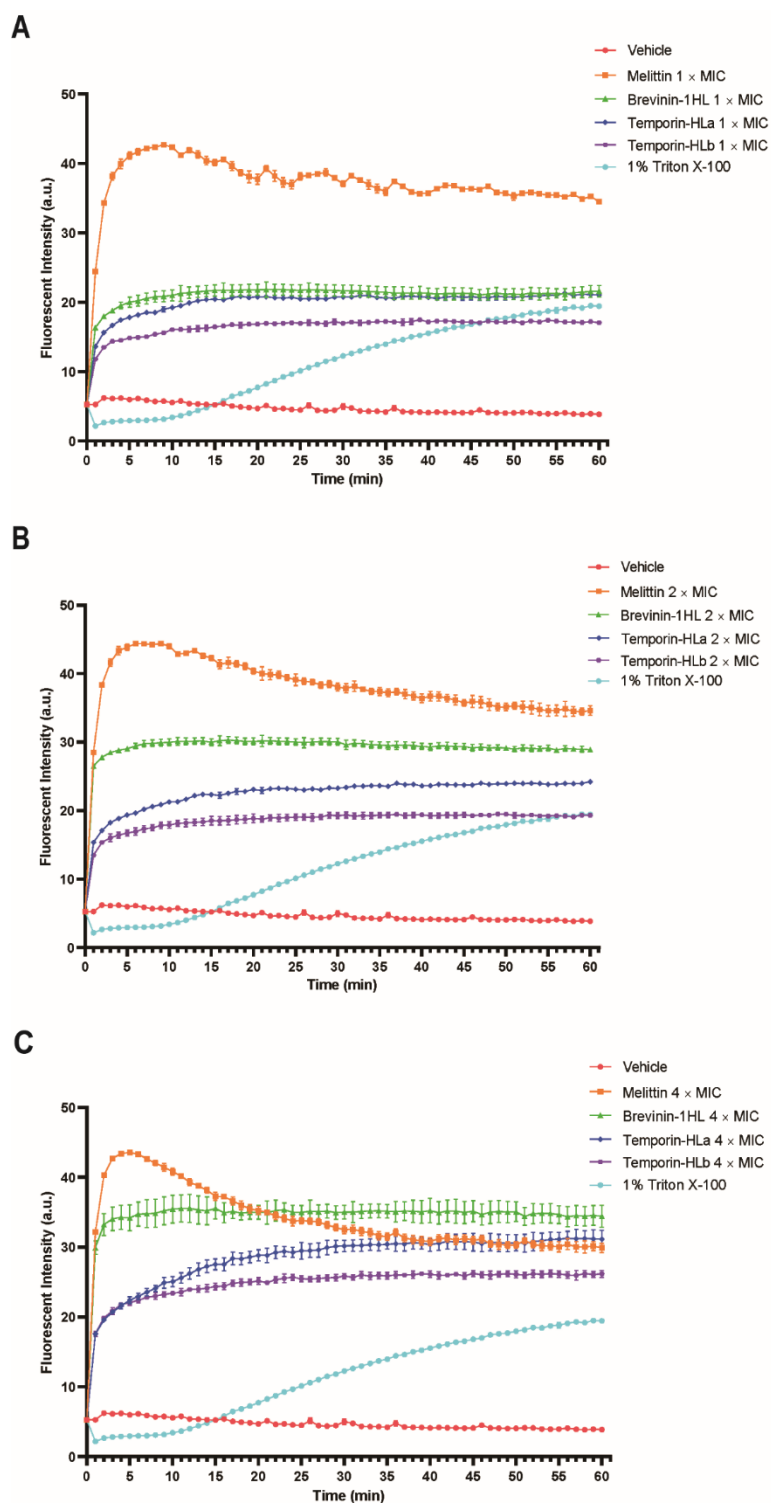


Figure 8,9), all the three peptides were able to permeabilise the bacterial membranes at 1× MICs in a very short time (5-30 min), and permeabilisation took place more rapidly and remarkably with the increase of concentrations. It was

deduced that under higher concentrations, the threshold could be achieved more quickly, forming a positive curvature on the membrane and inducing a severe cell damage with the carpet-like mechanism [49]. Direct observation of the impacts of peptides on the bacterial morphology with SEM confirmed the permeability and bacteriolysis of peptides on the test microorganisms (**Figure 10**). Additionally, it was found that it took more time for brevinin-1HL and melittin to induce an obvious penetrative procedure on Gram-negative bacterium (*E. coli*) and full destruction of the inner membrane was not accomplished within 150 min (**Figure 9A**), which could be explained by the theory that Gram-negative bacteria possess an extra outer membrane which makes it more difficult to be destroyed [50]. In the DNA binding assay, brevinin-1HL and temporin-HLa were found to be able to bind to the genomic DNAs of some sensitive microbes at high concentrations (**Figure 11**), indicating that they might also cause bacteria death by changing the DNA structures, interfering with gene expression and further affecting biological processes [51]. Thus, brevinin-1HL and temporin-HLa could kill bacteria by destroying the cell membranes, leading to cell lysis, and by binding to intracellular DNA, disturbing biological functions, while temporin-HLb inhibited the growth of bacteria mainly through the membrane permeabilisation ability.

Because the cytotoxic effects of AMPs on target cells are commonly related to their secondary structures and physicochemical properties, these characteristics of the peptides were examined by CD spectrometry and bioinformatics tools. Some studies revealed that a cationic charge and an amphipathic conformation are vital factors required by a broad range of AMPs for their activity [52]. Relevant results in this study (**Figure 5,6** and Error! Reference source not found.) suggested that the three peptides fit with the elementary requirements for the antimicrobial effects. Based on the calculated hydrophobicity shown in Error! Reference source not found., the higher hydrophobicity of temporin-HLa and -HLb might explain the decrease of antimicrobial activity, since increase in hydrophobicity might lead to the enhancement of peptide self-association to some extent, reducing the ability to penetrate cell membranes and cell walls [53].

The structures and physicochemical properties of the peptides most similar to brevinin-1HL, temporin-HLa and -HLb are also presented in Error! Reference source not found., to preliminarily reveal their structure-activity relationships. For

brevinin-1HL, the “Rana-box” seems to serve as a C-terminal cap to stabilise the helical structure, and additionally the formative disulphide bond can provide a resistance to proteases such as carboxypeptidase Y. The two positively-charged lysines within the “Rana-box” would favour its electrostatic interaction with the negatively-charged bacterial surface. According to its predicted 3D model and secondary structure (**Figure 6A** and Error! Reference source not found.), Pro¹⁴ located in the middle of the sequence could act as a helical kink, facilitating a diagonal binding of the peptides within membranes that forced the N-terminal helix to insert deeply into the core of the membrane to promote transmembrane pore formation, and the C-terminal helix helped the attachment to the lipid surface [54]. As shown in Error! Reference source not found., brevinin-1GHa and gaegurin 5 have about one more net positive charge (+4.9 and +5) than brevinin-1HL (+4), which may explain their distinct increase in antimicrobial activity as the increase in cationicity is generally correlated with the enhancement in antimicrobial activity [4,11,36,37,53].

For temporin-HLa and its similar peptides, the order of hydrophobicity and amphipathicity is temporin-HLa > temporin-LTa > temporin-RN1 > temporin-RN3 (Error! Reference source not found.), yet the antimicrobial potency and spectrum do not follow this order [34,35], indicating that the high value of some structural parameters is not enough for the best antimicrobial activity; instead, optimal balance in structural parameters is required for this.

For temporin-HLb, unlike the majority of AMPs which are usually positively-charged through the presence of basic Lys or Arg residues, only the free N-terminal amino group, C-terminal amide and two histidines at position 4 and 11 provide a total net charge of +1.2 to it (Error! Reference source not found.). The CD spectrum revealed that it adopted a classical amphipathic α -helical conformation (**Figure 5B**). Surprisingly, despite the extremely low positive net charge of temporin-HLb and its analogues (Error! Reference source not found.), they exhibited selective and even broad-spectrum antimicrobial activity [33]. Such results proved the crucial role of amphipathic α -helical conformation in AMPs activity towards target cells; a positive net charge of +1.2 without any basic amino acid residue is enough for AMPs to inhibit microorganisms.

It has been reported that some AMPs possess additional anticancer abilities due to some similar mechanisms of action towards bacterial and cancer cells [11–14]. In

terms of the anti-cancer activity of the three AMPs, temporin-HLa inhibited the proliferation of H23, H157 and H460 cancer cells (**Figure 12B-D**). H23 cells seemed to be more vulnerable to brevinin-1HL-induced cytotoxicity than other test cells (**Figure 12A**), yet temporin-HLb was devoid of toxicity on the cell lines tested (data not shown). The variable sensitivities of different cancer cell lines towards a given peptide may be attributed to the difference in cell membrane components such as the presence of anionic phosphatidylserine and O-glycosylated mucins which are believed to play key roles in promoting electrostatic interaction between AMPs and cancer cell surfaces, or because of the differences in cell membrane fluidity or surface area [14,55]. The low positive net charge of temporin-HLb and the resulting weak electrostatic interaction with cancer cells may explain its lack of anticancer activity. In addition, temporin-HLa only presented selective inhibitory activity towards Gram-positive bacteria and fungi but it possessed relatively broader anticancer spectrum than brevinin-1HL (Error! Reference source not found.-5). The different potencies of an AMP towards microorganisms and cancer cells may be due to some potentially different mechanisms. Although it is unclear why some AMPs have additional antitumour effects while others do not and it is also unknown if the molecular mechanisms behind the antimicrobial and anticancer activities of AMPs are the same or different [55], more extensive studies on the mechanisms of AMPs action would facilitate a better understanding in this respect. More significantly, a host of discovered AMPs may hold the answers to these questions and may prove to be promising candidates for novel natural source antimicrobial and anticancer agents which may overcome the shortcomings of conventional chemotherapy due to their high degree of selective cytotoxicity towards bacterial and neoplastic cells and an avoidance of multidrug resistance.

In conclusion, this study reports the identification, characterisation and biological investigations of three AMPs, namely brevinin-1HL, temporin-HLa and temporin-HLb, from the skin secretion of *H. latouchii*. They presented an α -helical structure, and possessed different inhibitory potencies towards test microorganisms and human cancer cell lines, causing varying cytotoxicity on horse red blood cells. They could cause prompt bacteria death by destroying the cell membranes, and brevinin-1HL and temporin-HLa could also penetrate the bacterial cell membranes to bind with the genomic DNA. The preliminary structure-activity studies may facilitate

rational design of each peptide for the development of novel antibacterial and antitumour drugs in the future to overcome the multidrug resistance and side-effects of chemotherapeutic agents. The sequence homology of brevinin-1 biosynthetic precursors from *H. latouchii* and *H. guentheri* continues to provide an insight into the elucidation of the evolutionary relationship and taxonomy of these two species.

Funding

This work was supported by the grants from the Natural Science Foundation of Fujian Province (No. 2019J01408), the Outstanding Young Scientist Program of Fujian Agriculture and Forestry University (No. xjq201916), and the National Natural Science Foundation of China (No. 31500753).

References

1. Rollins-Smith LA, Reinert LK, O’Leary CJ, Houston LE, Woodhams DC. Antimicrobial peptide defenses in amphibian skin. *Integr Comp Biol* 2005, 45: 137–142.
2. Hancock RE, Chapple DS. Peptide antibiotics. *Antimicrob Agents Chemother* 1999, 43: 1317–1323.
3. Conlon JM, Kolodziejek J, Nowotny N. Antimicrobial peptides from ranid frogs: taxonomic and phylogenetic markers and a potential source of new therapeutic agents. *Biochim Biophys Acta* 2004, 1696: 1–14.
4. Jiang Y, Wu Y, Wang T, Chen X, Zhou M, Ma C, Xi X, *et al.* Brevinin-1GHd: a novel *Hylarana guentheri* skin secretion-derived Brevinin-1 type peptide with antimicrobial and anticancer therapeutic potential. *Biosci Rep* 2020, 40: BSR20200019.
5. Wang H, He H, Chen X, Zhou M, Wei M, Xi X, Ma C, *et al.* A novel antimicrobial peptide (Kassinatuerin-3) isolated from the skin secretion of the African frog, *Kassina senegalensis*. *Biology (Basel)* 2020, 9: 148.
6. Li M, Xi X, Ma C, Chen X, Zhou M, Burrows JF, Chen T, *et al.* A novel dermaseptin isolated from the skin secretion of phyllomedusa tarsius and its cationicity-enhanced analogue exhibiting effective antimicrobial and anti-proliferative activities. *Biomolecules* 2019, 9: 628.
7. Chen D, Zhou X, Chen X, Huang L, Xi X, Ma C, Zhou M, *et al.* Evaluating the

- bioactivity of a novel antimicrobial and anticancer peptide, dermaseptin-PS4 (Der-PS4), from the skin secretion of *Phyllomedusa sauvagii*. *Molecules* 2019, 24: 2974.
8. Yu R, Wang M, Wang M, Han L. Melittin suppresses growth and induces apoptosis of non-small-cell lung cancer cells via down-regulation of TGF- β -mediated ERK signal pathway. *Braz J Med Biol Res* 2020, 54: e9017.
 9. Dong J, Tong S, Shi X, Wang C, Xiao X, Ji W, Sun Y. Progastrin-releasing peptide precursor and neuron-specific enolase predict the efficacy of first-line treatment with epidermal growth factor receptor (EGFR) tyrosine kinase inhibitors among non-small-cell lung cancer patients harboring EGFR mutations. *Cancer Manag Res* 2021, 12: 13607–13616.
 10. Papo N, Shai Y. Host defense peptides as new weapons in cancer treatment. *Cell Mol Life Sci* 2005, 62: 784–790.
 11. Yeaman MR, Yount NY. Mechanisms of antimicrobial peptide action and resistance. *Pharmacol Rev* 2003, 55: 27–55.
 12. Shai Y. Mode of action of membrane active antimicrobial peptides. *Biopolymers* 2002, 66: 236–248.
 13. Oren Z, Shai Y. Mode of action of linear amphipathic alpha-helical antimicrobial peptides. *Biopolymers* 1998, 47: 451–463.
 14. Schweizer F. Cationic amphiphilic peptides with cancer-selective toxicity. *Eur J Pharmacol* 2009, 625: 190–194.
 15. Wang C, Tian L, Li S, Li H, Zhou Y, Wang H, Yang Q, *et al.* Rapid cytotoxicity of antimicrobial peptide tempoprin-1CEa in breast cancer cells through membrane destruction and intracellular calcium mechanism. *PLoS One* 2013, 8: e60462.
 16. Hariton-Gazal E, Feder R, Mor A, Graessmann A, Brack-Werner R, Jans D, Gilon C, *et al.* Targeting of nonkaryophilic cell-permeable peptides into the nuclei of intact cells by covalently attached nuclear localization signals. *Biochemistry* 2002, 41: 9208–9214.
 17. Mai JC, Mi Z, Kim SH, Ng B, Robbins PD. A proapoptotic peptide for the treatment of solid tumors. *Cancer Res* 2001, 61: 7709–7712.
 18. Tyler MJ, Stone DJ, Bowie JH. A novel method for the release and collection of dermal, glandular secretions from the skin of frogs. *J Pharmacol Toxicol Methods* 1992, 28: 199–200.

19. Lin Y, Hang H, Chen T, Zhou M, Wang L, Shaw C. pLR-HL: a novel amphibian bowman-birk-type trypsin inhibitor from the skin secretion of the broad-folded frog, *Hylarana latouchii*. *Chem Biol Drug Des* 2016, 87: 91–100.
20. Vanhoye D, Bruston F, Nicolas P, Amiche M. Antimicrobial peptides from hylid and ranin frogs originated from a 150-million-year-old ancestral precursor with a conserved signal peptide but a hypermutable antimicrobial domain. *Eur J Biochem* 2003, 270: 2068–2081.
21. Shao C, Tian H, Wang T, Wang Z, Chou S, Shan A, Cheng B. Central β -turn increases the cell selectivity of imperfectly amphipathic α -helical peptides. *Acta Biomaterialia* 2018, 69: 243–255.
22. Kim H, Jang JH, Kim SC, Cho JH. De novo generation of short antimicrobial peptides with enhanced stability and cell specificity. *J Antimicrob Chemother* 2014, 69: 121–132.
23. Gautier R, Douguet D, Antony B, Drin G. HELIQUEST: a web server to screen sequences with specific α -helical properties. *Bioinformatics* 2008, 24: 2101–2102.
24. Yang J, Zhang Y. I-TASSER server: new development for protein structure and function predictions. *Nucleic Acids Res* 2015, 43: W174–181.
25. Lin Y, Hu N, Lyu P, Ma J, Wang L, Zhou M, Guo S, *et al.* Hylaranins: prototypes of a new class of amphibian antimicrobial peptide from the skin secretion of the oriental broad-folded frog, *Hylarana latouchii*. *Amino Acids* 2014, 46: 901–909.
26. Mokhtar JA, McBain AJ, Ledder RG, Binsuwaidan R, Rimmer V, Humphreys GJ. Exposure to a manuka honey wound gel is associated with changes in bacterial virulence and antimicrobial susceptibility. *Front Microbiol* 2020, 11: 2036.
27. Chen X, Zhang L, Wu Y, Wang L, Ma C, Xi X, Bininda-Emonds OR, *et al.* Evaluation of the bioactivity of a mastoparan peptide from wasp venom and of its analogues designed through targeted engineering. *Int J Biol Sci* 2018, 14: 599–607.
28. He H, Chen Y, Ye Z, Chen X, Ma C, Zhou M, Xi X, *et al.* Modification and targeted design of N-terminal truncates derived from brevinin with improved therapeutic efficacy. *Biology* 2020, 9: 209.
29. Helander IM, Mattila-Sandholm T. Fluorometric assessment of gram-negative bacterial permeabilization. *J Appl Microbiol* 2000, 88: 213–219.
30. Zhou X, Liu Y, Gao Y, Wang Y, Xia Q, Zhong R, Ma C, *et al.* Enhanced

- antimicrobial activity of N-terminal derivatives of a novel brevinin-1 peptide from the skin secretion of *Odorrana schmackeri*. *Toxins* 2020, 12: 484.
31. Zhong C, Zhang F, Yao J, Zhu Y, Zhu N, Zhang Y, Liu H, *et al.* Antimicrobial peptides with symmetric structures against multidrug-resistant bacteria while alleviating antimicrobial resistance. *Biochem Pharmacol* 2021, 186: 114470.
 32. Abbassi F, Oury B, Blasco T, Sereno D, Bolbach G, Nicolas P, Hani K, *et al.* Isolation, characterization and molecular cloning of new temporins from the skin of the North African ranid *Pelophylax saharica*. *Peptides* 2008, 29: 1526–1533.
 33. Dong Z, Luo W, Zhong H, Wang M, Song Y, Deng S, Zhang Y. Molecular cloning and characterization of antimicrobial peptides from skin of *Hylarana guentheri*. *Acta Biochim Biophys Sin* 2017, 49: 450–457.
 34. Wang H, Lu Y, Zhang X, Hu Y, Yu H, Liu J, Sun J. The novel antimicrobial peptides from skin of Chinese broad-folded frog, *Hylarana latouchii* (Anura:Ranidae). *Peptides* 2009, 30: 273–282.
 35. Ma Y, Liu C, Liu X, Wu J, Yang H, Wang Y, Li J, *et al.* Peptidomics and genomics analysis of novel antimicrobial peptides from the frog, *Rana nigrovittata*. *Genomics* 2010, 95: 66–71.
 36. Park JM, Jung JE, Lee BJ. Antimicrobial peptides from the skin of a Korean frog, *Rana rugosa*. *Biochem Biophys Res Commun* 1994, 205: 948–954.
 37. Chen Q, Cheng P, Ma C, Xi X, Wang L, Zhou M, Bian H, *et al.* Evaluating the bioactivity of a novel broad-spectrum antimicrobial peptide brevinin-1GHa from the frog skin secretion of *Hylarana guentheri* and its analogues. *Toxins (Basel)* 2018, 10: 413.
 38. Matsuzaki K. Control of cell selectivity of antimicrobial peptides. *Biochim Biophys Acta* 2009, 1788: 1687–1692.
 39. Giuliani A, Pirri G, Nicoletto SF. Antimicrobial peptides: an overview of a promising class of therapeutics. *Cent Eur J Biol* 2007, 2: 1–33.
 40. Li J, Xu X, Xu C, Zhou W, Zhang K, Yu H, Zhang Y, *et al.* Anti-infection peptidomics of amphibian skin. *Mol Cell Proteomics* 2007, 6: 882–894.
 41. B Bevens CL, Zasloff M. Peptides from frog skin. *Annu Rev Biochem* 1990, 59: 395–414.
 42. Simmaco M, Mignogna G, Barra D. Antimicrobial peptides from amphibian skin: what do they tell us? *Biopolymers* 1998, 47: 435–450.

43. Haney EF, Hunter HN, Matsuzaki K, Vogel HJ. Solution NMR studies of amphibian antimicrobial peptides: linking structure to function? *Biochim Biophys Acta* 2009, 1788: 1639–1655.
44. Gong Z, Pei X, Ren S, Chen X, Wang L, Ma C, Xi X, *et al.* Identification and rational design of a novel antibacterial peptide dermaseptin-AC from the skin secretion of the red-eyed tree frog *Agalychnis callidryas*. *Antibiotics (Basel)* 2020, 9: 243.
45. Chan DI, Prenner EJ, Vogel HJ. Tryptophan- and arginine-rich antimicrobial peptides: structures and mechanisms of action. *Biochim Biophys Acta* 2006, 1758: 1184–1202.
46. Saravanan R, Joshi M, Mohanram H, Bhunia A, Mangoni ML, Bhattacharjya S. NMR structure of temporin-1 ta in lipopolysaccharide micelles: mechanistic insight into inactivation by outer membrane. *PLoS One* 2013, 8: e72718.
47. Hall CW, Mah TF. Molecular mechanisms of biofilm-based antibiotic resistance and tolerance in pathogenic bacteria. *FEMS Microbiol Rev* 2017, 41: 276–301.
48. Zhou X, Shi D, Zhong R, Ye Z, Ma C, Zhou M, Xi X, *et al.* Bioevaluation of ranatuerin-2Pb from the frog skin secretion of *Rana pipiens* and its truncated analogues. *Biomolecules* 2019, 9: 249.
49. Rasamiravaka T, Labtani Q, Duez P, El Jaziri M. The formation of biofilms by *Pseudomonas aeruginosa*: a review of the natural and synthetic compounds interfering with control mechanisms. *Biomed Res Int* 2015, 2015: 759348.
50. Putker F, Bos MP, Tommassen J. Transport of lipopolysaccharide to the Gram-negative bacterial cell surface. *FEMS Microbiol Rev* 2015, 39: 985–1002.
51. Dong W, Luo X, Sun Y, Li Y, Wang C, Guan Y, Shang D. Binding Properties of DNA and Antimicrobial peptide chensinin-1b containing lipophilic alkyl tails. *J Fluoresc* 2020, 30: 131–142.
52. Powers JPS, Hancock REW. The relationship between peptide structure and antibacterial activity. *Peptides* 2003,24: 1681–1691.
53. Chen Y, Guarnieri MT, Vasil AI, Vasil ML, Mant CT, Hodges RS. Role of peptide hydrophobicity in the mechanism of action of alpha-helical antimicrobial peptides. *Antimicrob Agents Chemother* 2007, 51: 1398–1406.
54. Won HS, Kang SJ, Lee BJ. Action mechanism and structural requirements of the antimicrobial peptides, gaegurins. *Biochim Biophys Acta* 2009, 1788:

1620–1629.

55. Hoskin DW, Ramamoorthy A. Studies on anticancer activities of antimicrobial peptides. *Biochim Biophys Acta* 2008, 1778: 357–375.

Table 1. The observed and calculated molecular masses of three peptides (brevinin-1HL, temporin-HLa, and temporin-HLb), and reverse phase HPLC fractions

of *H. latouchii* skin secretion in which they were located.

Peptide	Original fraction	Mass observed (Da)	Mass calculated (Da)
Brevinin-1HL	125	2495.45	2495.14
Temporin-HLa	153	1876.64	1875.38
Temporin-HLb	131	1496.46	1494.81

Table 2. Structures and some physicochemical properties of the peptides.

Peptides	Secondary structures	Net charge	Hydrophobicity <H>	Hydrophobic moment <μH>
Brevinin-1HL	FLGALFKVASKLVPAAICSISKKC cchhhhhhhhhhhcchhhhhhhceccc	+4	0.653	0.364
Brevinin-1GHa [37]	FLGAVLKVAGKLVPAAICKISKKC cchhhhhhhhhcchhhhhhhceccc	+4.9	0.592	0.358
Gaegurin 5 [36]	FLGALFKVASKVLPVSKCAITKKC cchhhhhhhhhccccsssscecc	+5	0.588	0.376
Temporin-HLa	FFPLIFGALSSILPKIL cchhhhhhhhhhhhhhhcc	+2	1.074	0.496
Temporin-RN1 [35]	FLPLVLGALSGILPKIL cccchhhhhhhceccc	+2	1.031	0.461
Temporin-RN3 [35]	FFPLIFGALSSHLPKLF cchhhhhhhhhhhceccc	+2.1	0.969	0.453
Temporin-LTa [34]	FFPLVLGALGSILPKIF cccchhhhhhhhhceccc	+2	1.042	0.470
Temporin-HLb	FLQHIIGALSHIF chhhhhhhhhhhcc	+1.2	0.976	0.632
Temporin-GHc [33]	FLQHIIGALTHIF chhhhhhhhhhhcc	+1.2	0.999	0.623
Temporin-GHd [33]	FLQHIIGALSHFF chhhhhhhhhhhcc	+1.2	0.975	0.631
Temporin-GHa [33]	FLQHIIGALGHLF chhhhhhhhhhhcc	+1.2	0.972	0.625

Table 3. MICs and MBCs of peptides against model test microorganisms.

Peptide	Activities	<i>E. coli</i>	<i>P. aeruginosa</i>	<i>C. violaceum</i>	<i>S. aureus</i>	MRSA	<i>E. faecalis</i>	<i>C. albicans</i>
Brevinin-1HL	MIC	128 mg/L (51.3 µM)	256 mg/L (102.6 µM)	>512 mg/L (205.2 µM)	8 mg/L (3.2 µM)	128 mg/L (51.3 µM)	32 mg/L (12.8 µM)	16 mg/L (6.4 µM)
	MBC	128 mg/L (51.3 µM)	>512 mg/L (205.2 µM)	>512 mg/L (205.2 µM)	32 mg/L (12.8 µM)	>512 mg/L (205.2 µM)	>512 mg/L (205.2 µM)	32 mg/L (12.8 µM)
	Haemolysis at MIC	82.4%	86.8%	-	19.7%	82.4%	53.0%	34.0%
	HC ₅₀	28.7 ± 0.6 mg/L (11.5 ± 0.2 µM)						
Temporin-HLa	MIC	>512 mg/L (273.1 µM)	>512 mg/L (273.1 µM)	>512 mg/L (273.1 µM)	16 mg/L (8.5 µM)	>512 mg/L (273.1 µM)	16 mg/L (8.5 µM)	32 mg/L (17.1 µM)
	MBC	>512 mg/L (273.1 µM)	>512 mg/L (273.1 µM)	>512 mg/L (273.1 µM)	64 mg/L (34.1 µM)	>512 mg/L (273.1 µM)	>512 mg/L (273.1 µM)	128 mg/L (68.3µM)
	Haemolysis at MIC	-	-	-	15.3%	-	15.3%	24.8%
	HC ₅₀	58.9 ± 1.3 mg/L (31.4 ± 0.7 µM)						
Temporin-HLb	MIC	>512 mg/L (342.7 µM)	>512 mg/L (342.7 µM)	>512 mg/L (342.7 µM)	16 mg/L (10.7 µM)	>512 mg/L (342.7 µM)	>512 mg/L (342.7 µM)	>512 mg/L (342.7 µM)
	MBC	>512 mg/L (342.7 µM)	>512 mg/L (342.7 µM)	>512 mg/L (342.7 µM)	>512 mg/L (342.7 µM)	>512 mg/L (342.7 µM)	>512 mg/L (342.7 µM)	>512 mg/L (342.7 µM)
	Haemolysis at MIC	-	-	-	1.0%	-	-	-
	HC ₅₀	27.8 ± 14.9 g/L (18.6 ± 10.0 mM)						
Melittin	MIC	16 mg/L (5.6 µM)	128 mg/L (45.0 µM)	>512 mg/L (179.9 µM)	8 mg/L (2.8 µM)	8 mg/L (2.8 µM)	8 mg/L (2.8 µM)	8 mg/L (2.8 µM)
	MBC	32 mg/L (11.2 µM)	128 mg/L (45.0 µM)	>512 mg/L (179.9 µM)	16 mg/L (5.6 µM)	16 mg/L (5.6 µM)	16 mg/L (5.6 µM)	16 mg/L (5.6 µM)
	Haemolysis at MIC	76.2%	97.0%	-	75.0%	75.0%	75.0%	75.0%
	HC ₅₀	0.37 ± 0.02 mg/L (0.130 ± 0.007 µM)						

Table 4. MBICs and MBECs of peptides against *P. aeruginosa* and *S. aureus*.

Peptide	Activities	<i>P. aeruginosa</i>	<i>S. aureus</i>
Brevinin-1HL	MBIC	256 mg/L (102.6 μ M)	64 mg/L (25.7 μ M)
	MBEC	>512 mg/L (205.2 μ M)	128 mg/L (51.3 μ M)
Temporin-HLa	MBIC	-	32 mg/L (17.1 μ M)
	MBEC	-	>512 mg/L (273.1 μ M)
Temporin-HLb	MBIC	-	32 mg/L (21.4 μ M)
	MBEC	-	>512 mg/L (342.7 μ M)
Melittin	MBIC	128 mg/L (45.0 μ M)	8 mg/L (2.8 μ M)
	MBEC	256 mg/L (90.0 μ M)	32 mg/L (11.2 μ M)

Table 5. IC₅₀ values of brevinin-1HL and temporin-HLa on H23, H157, and H460 cells after 24, 48, and 72 h of incubation.

	IC ₅₀ (μM)		
	24 h	48 h	72 h
Brevinin-1HL			
H23	8.52 ± 1.02	8.55 ± 1.79	8.62 ± 0.63
Temporin-HLa			
H23	4.96 ± 0.94	5.67 ± 0.20	6.74 ± 1.08
H157	15.18 ± 2.98	15.52 ± 2.19	13.56 ± 3.49
H460	1.64 ± 0.41	3.56 ± 0.53	3.27 ± 0.18

Figure legends

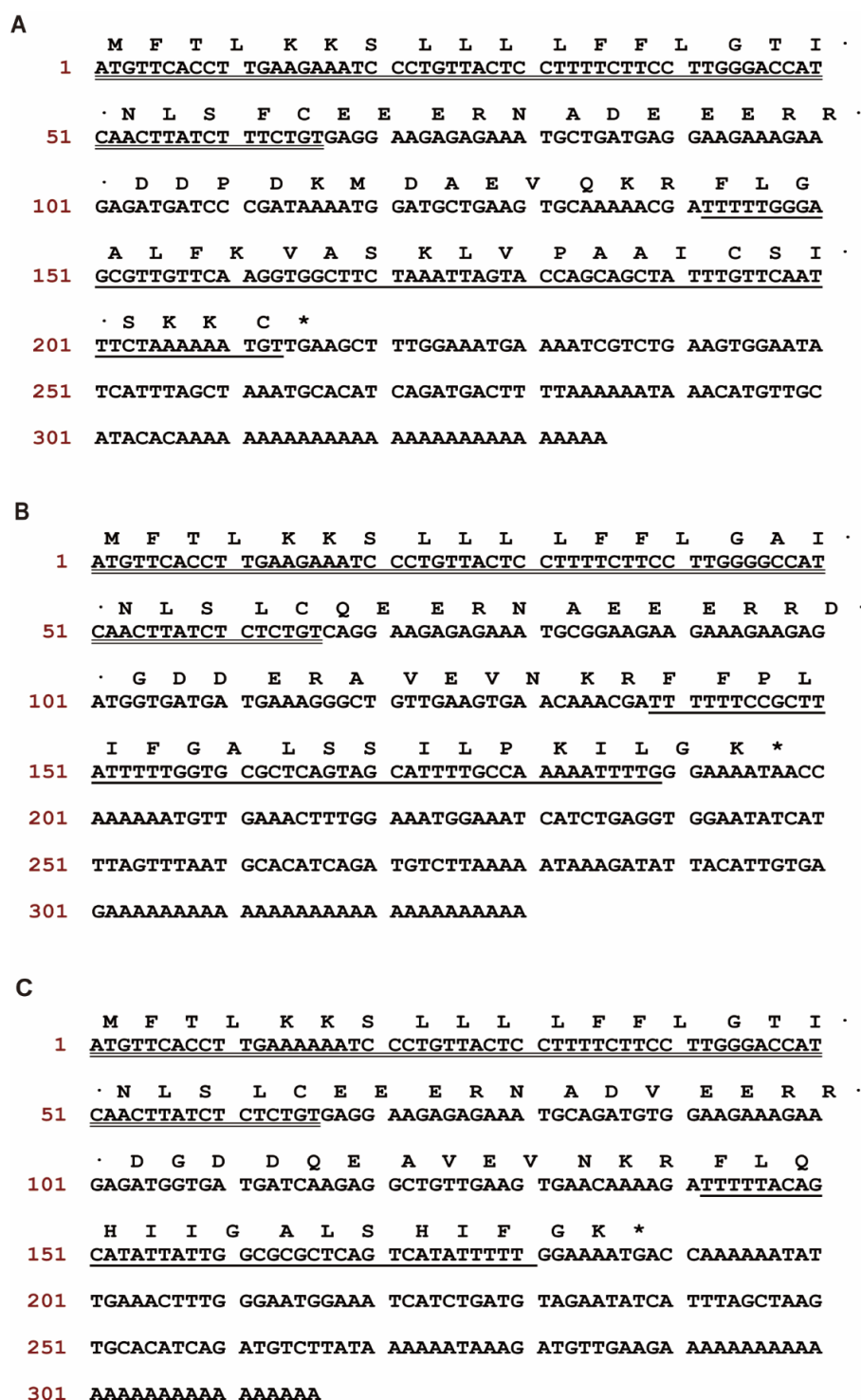


Figure 1. Nucleotides and translated amino acid sequences of the cDNAs encoding the prepropeptides of three peptides The putative signal peptides are double-underlined, the mature peptide sequences are single-underlined, and the stop codons are indicated by asterisks. (A) brevinin-1HL, (B) temporin-HLa, (C) temporin-HLb.

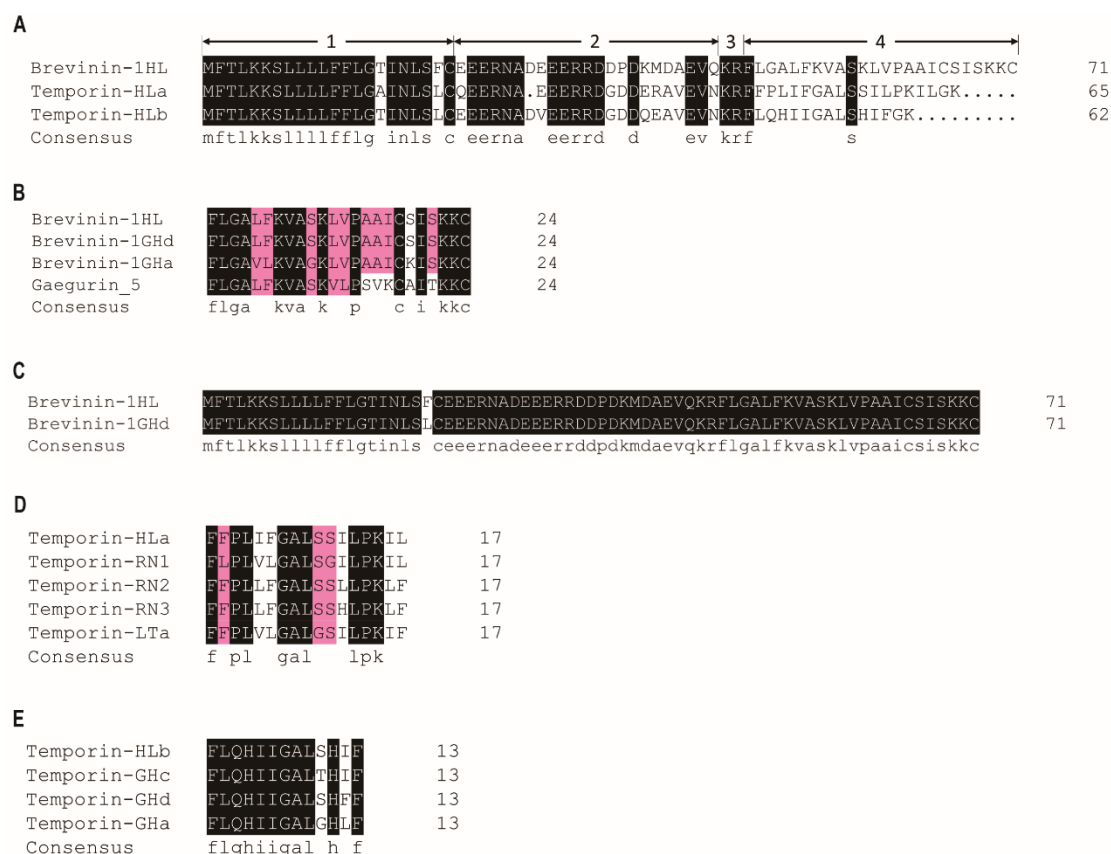


Figure 2. Alignments of three peptides and highly homologous peptides (A)

Alignments of the full open-reading frame amino acid sequences of brevinin-1HL, temporin-HLa and temporin-HLb precursors. Gaps have been included to maximise alignments. Identical residues are shaded in black and domain topologies are numbered. (1) Putative signal peptide; (2) acidic amino acid residue-rich spacer peptide; (3) classical propeptide convertase processing site (-KR-); (4) variable mature peptides including an amide donor (-GK-) for the C-terminal amidated residue of temporin-HLa and -HLb. Alignments of the mature (B) brevinin-1HL, (D) temporin-HLa, (E) temporin-HLb, and the (C) brevinin-1HL precursor with the peptides showing the highest sequence similarity through NCBI BLASTp search [33–37]. Identical residues are shaded in black and similar residues are shaded in pink.

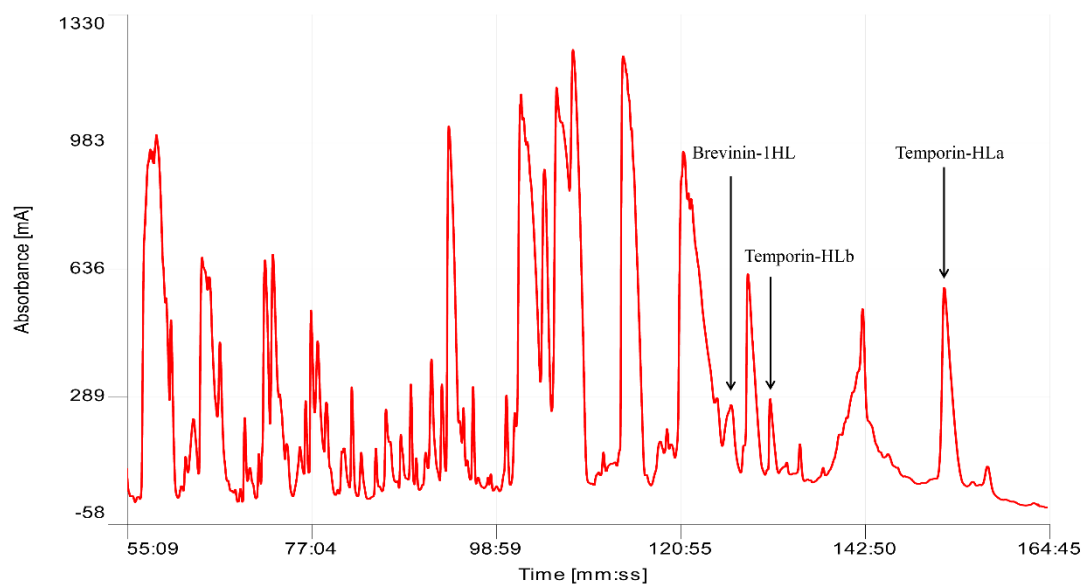


Figure 3. HPLC chromatogram of *H. latouchii* skin secretion indicating the elution time of brevinin-1HL, temporin-HLa and temporin-HLb

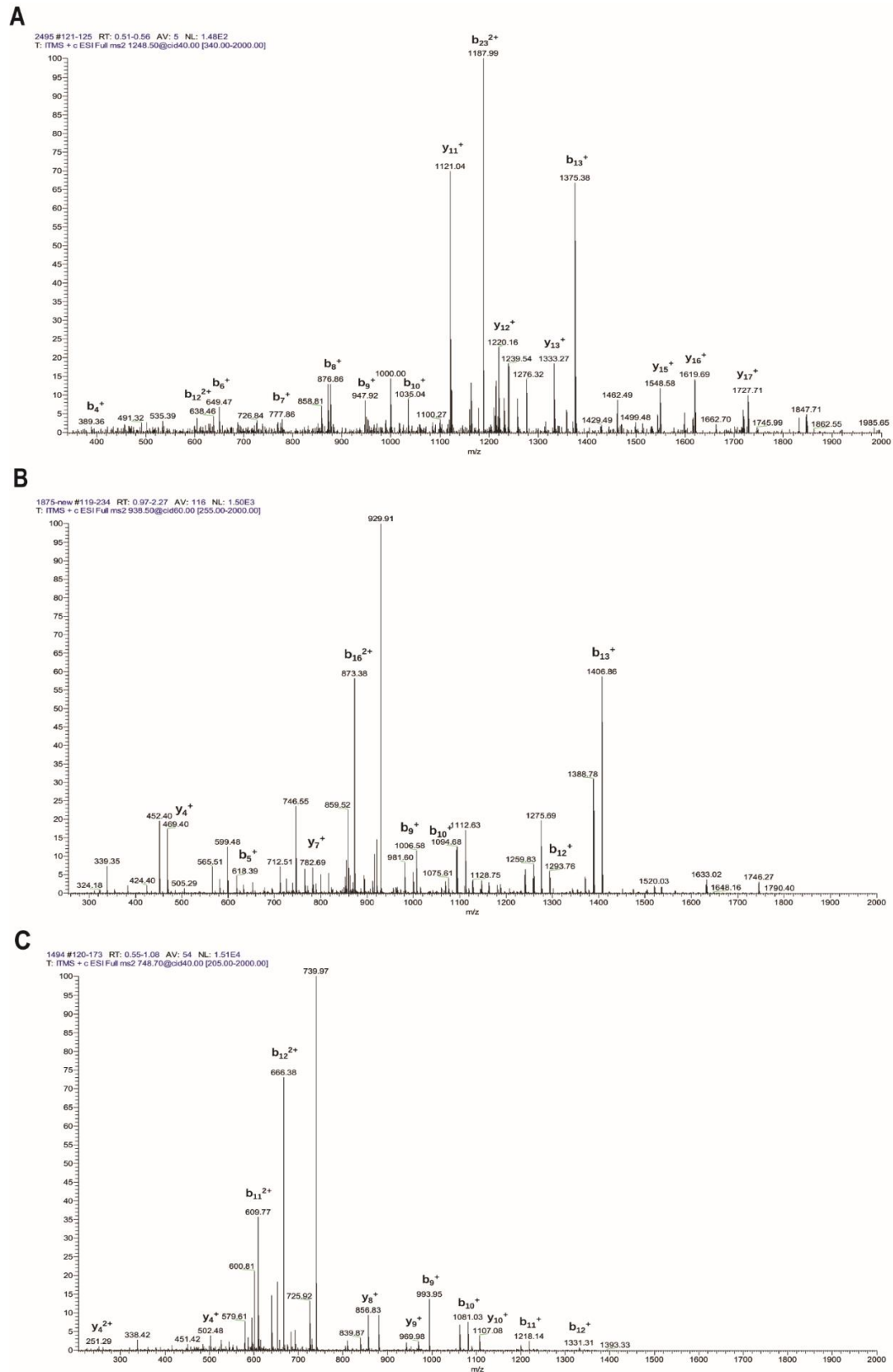


Figure 4. MS/MS fragmentation sequencing spectra of three peptide identified in the reverse phase HPLC fractions (A) brevini-1HL, (B) temporin-HLa, (C) temporin-HLb.

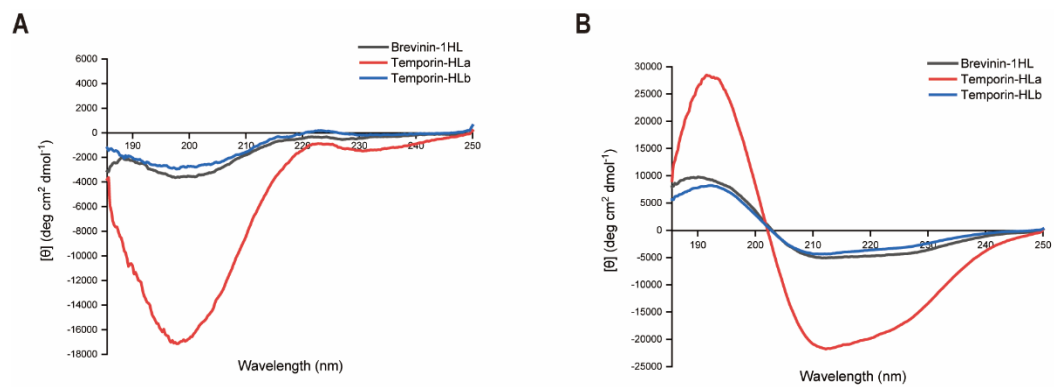


Figure 5. CD spectra of peptides in water and 50% TFE solution (A) water, (B) 50% TFE solution

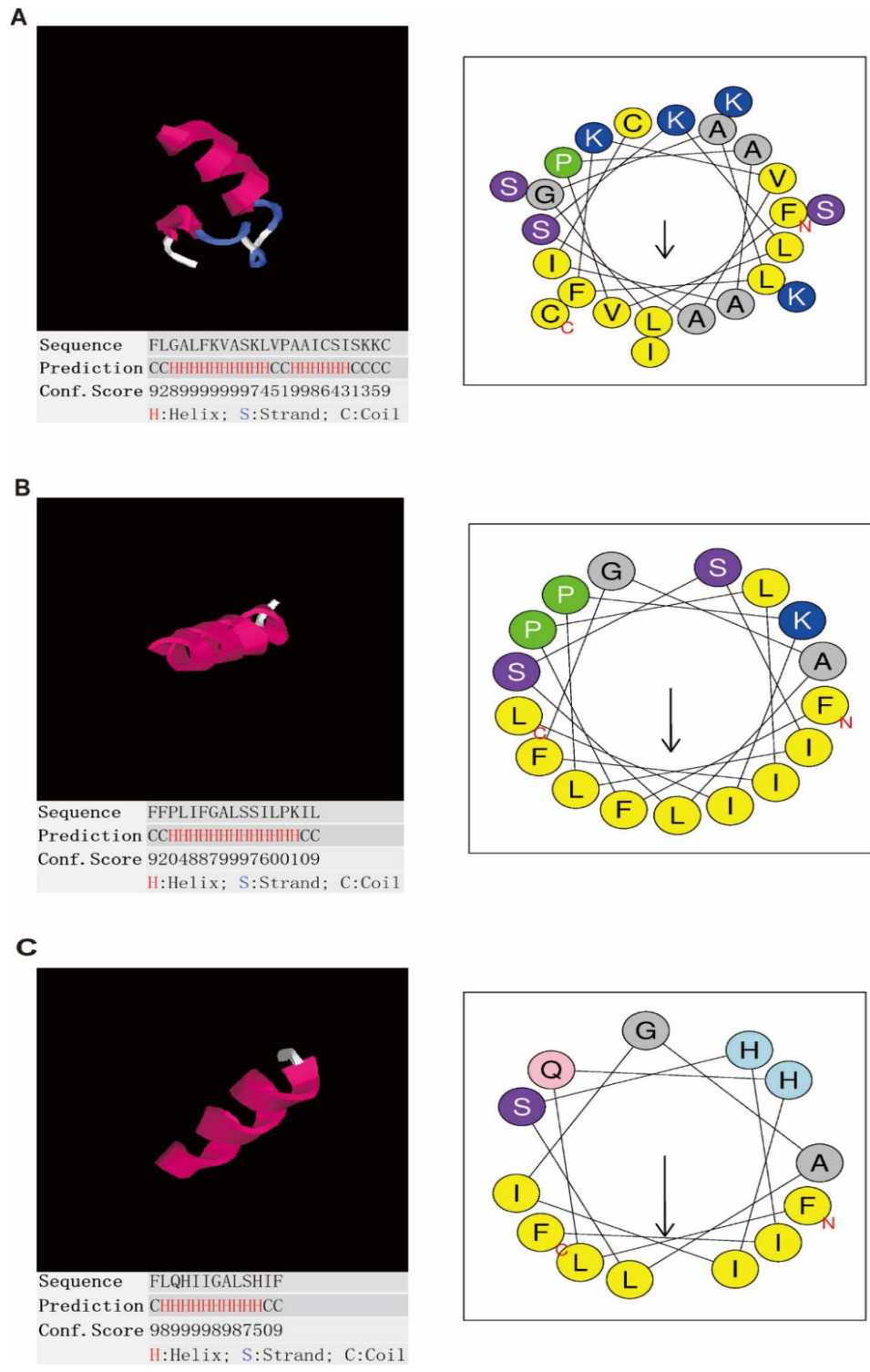


Figure 6. Secondary structure and 3D model predictions of three peptides 3D models are displayed on the left panels, and helical wheel plots are displayed on the right panels in which the positively charged, hydrophobic, hydrophilic, amide and small residues are indicated in blue, yellow, purple, pink and grey, respectively. Arrows indicate the hydrophobic face. (A) brevinin-1HL, (B) temporin-HLa, (C) temporin-HLb.

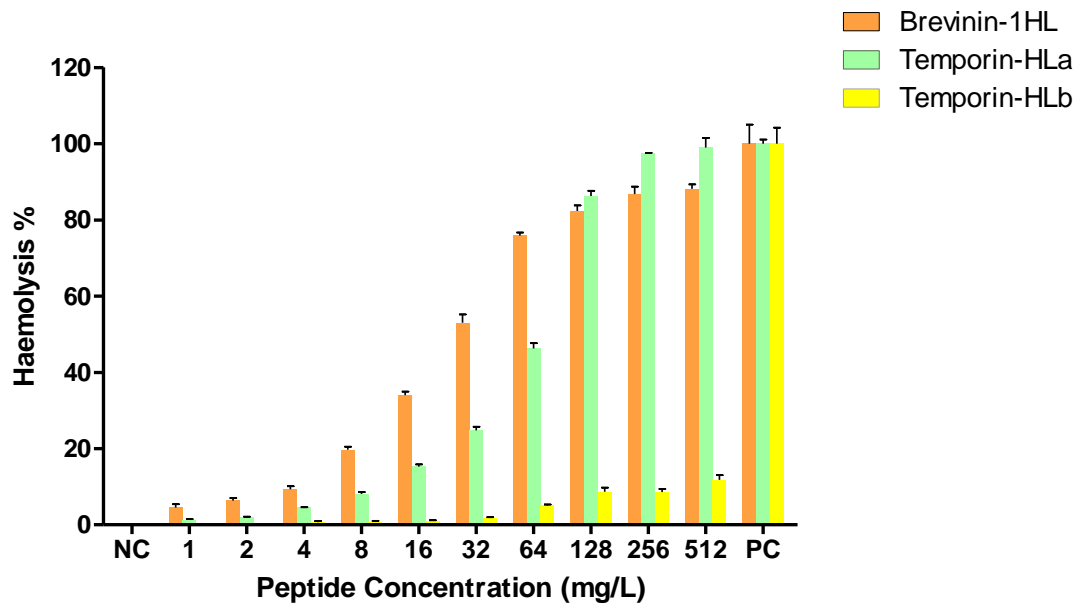


Figure 7. Haemolytic activities of three antimicrobial peptides on horse erythrocytes PC, positive control that horse erythrocytes incubated with 0.1% TritonX-100. NC, negative control that were incubated with PBS.

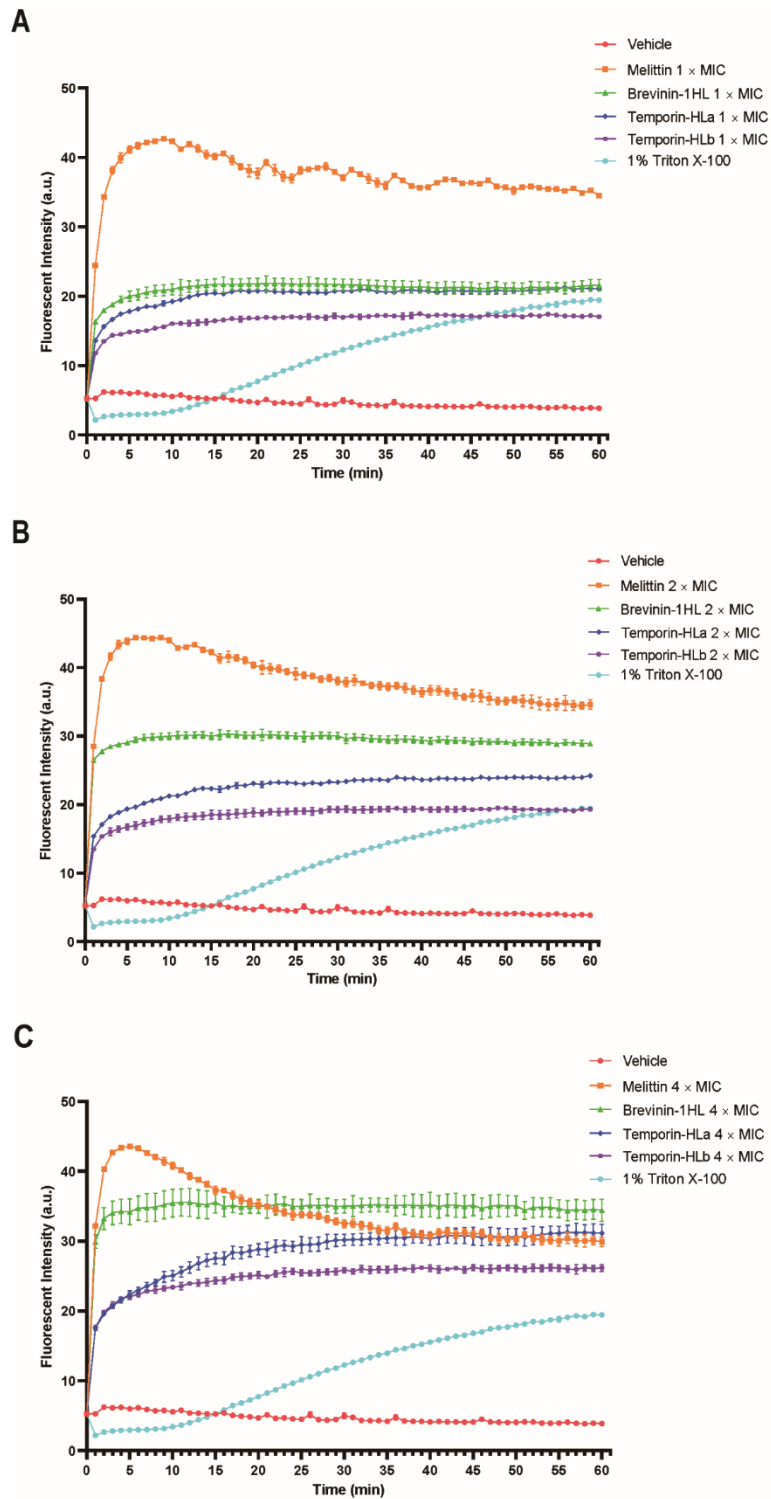


Figure 8. Changes in the membrane permeability of *S. aureus* treated with the peptides (A) 1 × MICs, (B) 2 × MICs and (C) 3 × MICs.

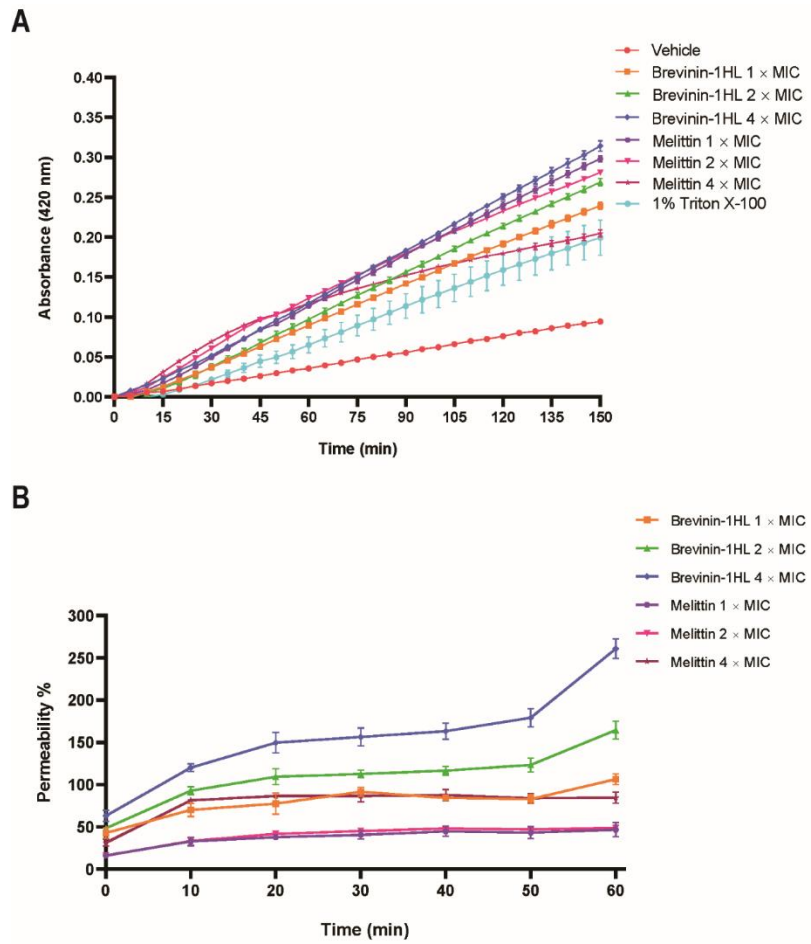


Figure 9. Changes in the membrane permeability of *E. coli* treated with brevinin-1HL (A) inner membrane, (B) outer membrane.

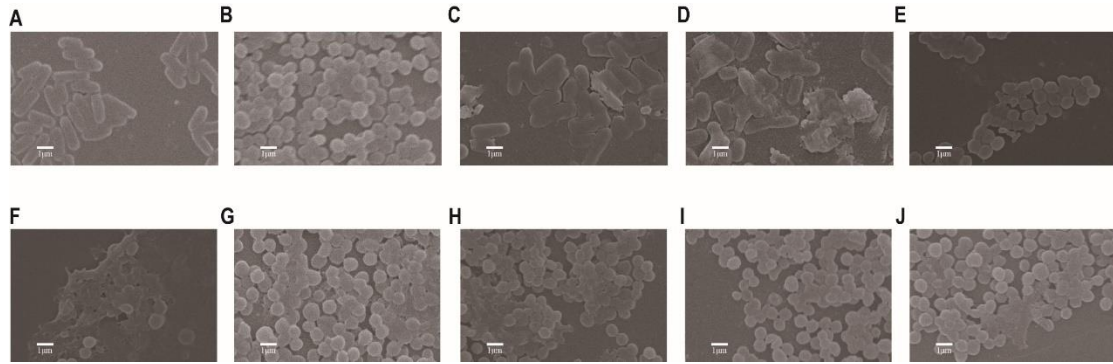


Figure 10. SEM micrographs of *E. coli* and *S. aureus* treated with peptides for 18 h Untreated (A) *E. coli* and (B) *S. aureus*. (C,D) *E. coli* treated with brevenin-1HL at $0.25 \times$ and $0.5 \times$ MICs. *S. aureus* treated with (E,F) brevenin-1HL, (G,H) temporin-HLa and (I,J) -HLb at $0.25 \times$ and $0.5 \times$ MICs.

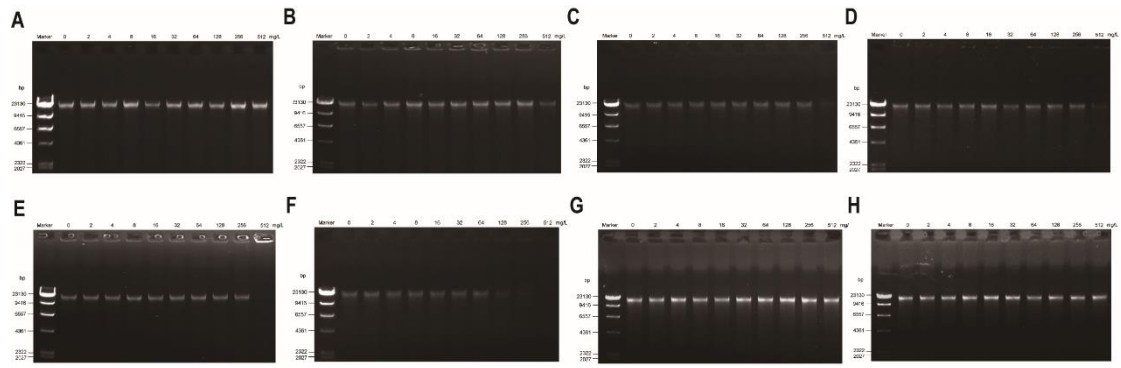


Figure 11. DNA binding ability of peptides to the sensitive microbes (A-E) Electrophoresis of brevinin-1HL binding to the genomic DNA of *E. coli*, *P. aeruginosa*, *S. aureus*, MRSA and *E. faecalis*. (F,G) DNA binding of temporin-HLA to *S. aureus* and *E. faecalis*. (H) DNA binding of temporin-HLb to *S. aureus*.

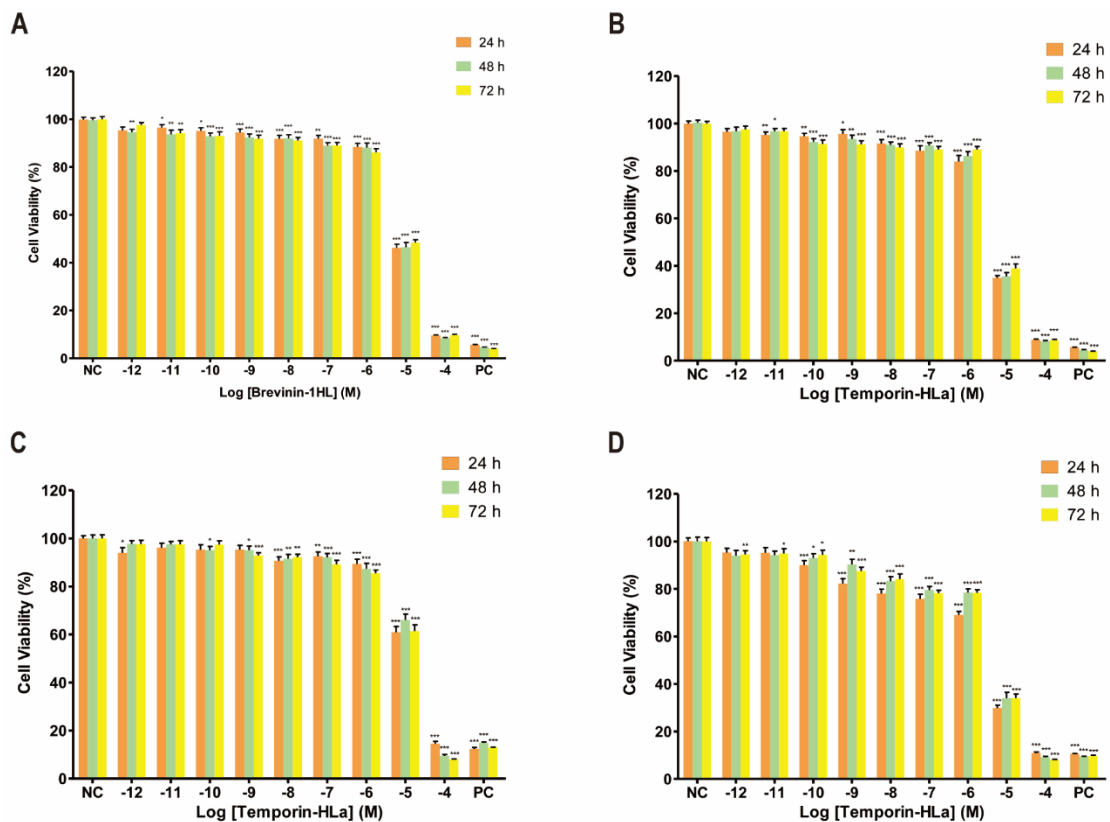


Figure 12. Anti-proliferative effects of brevinin-1HL and temporin-HL on human cancer cell lines (A) Anticancer effects of brevinin-1HL on H23 cells. (B-D) Anticancer effects of temporin-HL on H23, H157 and H460 cells, respectively. * $P < 0.05$, ** $P < 0.01$, *** $P < 0.001$, indicate statistical significance of differences versus control.